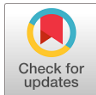

Research Article Vol. 29, No. 9 / 26 April 2021 / Optics Express 14058

Optics EXPRESS

Hydrostatic pressure effect of photocarrier dynamics in GaAs probed by time-resolved terahertz spectroscopy

HPSTAR 1269-2021

SHUJUAN XU,[1,2] DAJIAN HUANG,[3] ZHENG LIU,[1,4] KAI ZHANG,[1] HUACHAO JIANG,[1] HUIYANG GOU,[3] ZHI ZENG,[1] TIANWU WANG,[5,6] AND FUHAI SU[1,7]

[1] *Key Laboratory of Materials Physics, Institute of Solid State Physics, HFIPS, Chinese Academy of Sciences, Hefei 230031, China*
[2] *University of Science and Technology of China, Hefei 230026, China*
[3] *Center for High Pressure Science and Technology Advanced Research, Beijing 100094, China*
[4] *Institutes of Physical Science and Information Technology, Anhui University, Hefei 230601, China*
[5] *Great Bay Area Research Institute, Aerospace Information Research Institute (AIR) of Chinese Academy of Science (CAS), Guangzhou 510700, China*
[6] *wangtw@aircas.ac.cn*
[7] *fhsu@issp.ac.cn*

Abstract: Pressure effects on photocarrier dynamics such as interband relaxations and intraband cooling in GaAs have been investigated using in situ time-resolved terahertz spectroscopy with a diamond anvil cell. The interband photocarrier lifetime significantly decreases by nearly two orders of magnitude as the external hydrostatic pressure is increased up to 10 GPa. Considerable pressure tuning for the intervalley scattering processes has also been observed, and the time constants under different pressures are extracted based on the three-state rate model. This work provides new perspectives on tailoring nonequilibrium carrier dynamics in semiconductors using hydrostatic pressure and may serve as the impetus for the development of high-pressure terahertz spectroscopy.

© 2021 Optical Society of America under the terms of the OSA Open Access Publishing Agreement

1. Introduction

Because hot carriers with excess energy above the band extrema in semiconductors play an essential role in the photovoltaic and photothermoelectric effect, as well as high-field electron transport [1–3], tuning the dynamics of hot carriers has fundamental significance for the development of photoelectric and electric devices such as the terahertz (THz) emitter, light-harvesting, high-frequency electronics. For example, accelerating the cooling processes of photocarriers in semiconductors helps to optimize the efficiency and bandwidth of THz emission using defect engineering, including low-temperature grown molecular beam epitaxy (MBE) and radiation damage [4–6]. In contrast, reversing hot carriers via the intervalley scattering of satellite valleys [7] or the phonon bottleneck of high-energy carrier scattering [8–11], promises a significant increase in energy conservation efficiency in solar cells. The high-pressure technique based on the diamond anvil cell (DAC) provides a simple and clean route to tune the lattice and electronic structures [12], whereby pressure tuning on ultrafast dynamics including Auger recombination [13], thermal transport [14], and hot carrier cooling [15] has been achieved. GaAs, serving as a versatile platform, hosts intriguing ultrafast photophysics such as THz nonlinear absorption [16–18], and phonon-decoupling [19] as dictated by hot carriers. Indeed, it is the earlier investigations of photocarrier dynamics in GaAs that established the principles of hot carrier effects and the corresponding dynamic mechanisms [20,21]. Therefore, understanding

#421011 https://doi.org/10.1364/OE.421011
Journal © 2021 Received 29 Jan 2021; revised 7 Apr 2021; accepted 13 Apr 2021; published 23 Apr 2021

of photocarrier dynamics of GaAs under high pressure is expected to provide new insights to improve the photoelectric performance of semiconductor devices.

It is well known that GaAs, a typical direct gap semiconductor, has a conduction band (CB) composed of Γ, L and X satellite valleys. With the application of hydrostatic pressure, the Γ and L valley extrema move upward, however, the X valley minimum moves downward [22,23]. Above 4 GPa, a crossover between the Γ and X valley extrema occurs, forming an indirect bandgap at the X point. In earlier works [22,24–27], time-resolved photoluminescence spectroscopy was employed to study the interband recombination dynamics of GaAs under pressure. It was found that the lifetime of the shallow donor-exciton state increased remarkably as the Γ-X crossover occurred in p-type GaAs [25], while the recombination lifetime in n-type GaAs decreased [26,27] under hydrostatic pressure. In addition, Grivickas et al. [28] observed a linear order of magnitude lifetime reduction in n-type GaAs under uniaxial pressure produced by a shock wave. However, the ultrafast hot carrier cooling processes in picoseconds timescale, such as intervalley scattering and fast surface trapping in compressed GaAs have not yet been investigated.

Time-resolved terahertz spectroscopy (TRTS) has emerged as an ideal non-contact probe method for carrier dynamics with a subpicosecond temporal resolution, benefiting from simultaneous access to the frequency and time-resolved photoconductivities. This technique was first applied to the study of free carrier dynamics in GaAs [29–31] at ambient pressure. TRTS has facilitated the profound understanding of ultrafast photocarrier dynamics, including interband recombination, surface recombination, spatial diffusion, and intervalley scattering in GaAs [16,32]. However, as the THz beam with mm-scale spot size would be attenuated dramatically by the DAC with a small clear aperture, the application of in-situ TRTS under high pressure is currently limited. In this work, we investigate the photocarrier dynamics in GaAs under hydrostatic pressure using TRTS. Experimentally, a DAC is utilized to generate hydrostatic pressures up to 10 GPa. To overcome the huge attenuation from DAC, the intense THz pulses from a $LiNbO_3$ crystal are used as the probe in TRTS. Under pressure, the photocarrier lifetime corresponding to the interband relaxation is found to reduce to a few picoseconds, comparable with that in low-temperature-grown GaAs (LT-GaAs), from nanoseconds at ambient condition. This considerable decrease is attributed to a pressure-induced augmentation in the density of surface defect states. Pressure effects on the inter-valley scattering of hot carriers in GaAs have also been observed, consistent with the pressure evolution of energy band structures. This work provides new insights on tailoring the photocarrier dynamics in semiconductors using hydrostatic pressure, likely stimulating the development of high-pressure THz spectroscopy.

2. Experiments

A DAC with a culet size of 500 μm was used to exert external hydrostatic pressure (see Fig. 1(a)). The aperture of the drilled stainless steel gasket was about 300 μm in diameter. A piece of undoped GaAs single crystal wafer with <100> orientation was polished into a thin-platelet sample with a size around 200 × 150 μm and thickness of about 10 μm to be loaded in the DAC together with a ruby particle as shown in Fig. 1(b). Figure 1(c) shows the photograph of the sample in the DAC device. Silicone oil was used as a pressure transmitting medium (PTM), and the pressure was gauged using ruby fluorescence [12].

The experimental scheme was plotted in Fig. 1(c). A 1-kHz, 45-fs Ti: sapphire amplifier (Coherent Legend) was used as the laser source. The laser beam was divided into three portions for generating and sampling THz transients, as well as optical excitation of the sample inside the DAC, respectively. THz pulses with 500 *nJ* were generated in a $LiNbO_3$ prism using the tilted-pulse front technique [33,34]. Free-space electro-optic sampling was used to coherently detect the THz electric field transmitted through the DAC. The DAC chamber with the sample was globally illuminated by both THz and pump beams. The optical chopper was placed in either the THz generation path to detect the THz electric field waveform or the optical pump path to

record the photoinduced transmission change. Furthermore, the time evolution of differential transmission at the main peak of the THz pulse, $\Delta T/T_0 = (T_p - T_0)/T_0$, was recorded using a lock-in amplifier by varying the optical pump-THz probe delay and keeping the delay of optical gating pulse with respect to the THz pulse fixed. Here, T_p and T are the transmissions at THz peak with and without photoexcitation, respectively. The output of an equipped optical parameter amplifier (OPA) at 600 nm was also used as a pump beam. In the following, the pump laser for photoexcitation was at an 800 nm wavelength unless otherwise specified. All the TRTS experiments were performed at room temperature. In the measurements, the applied pump fluences were kept below 60 μJ/cm^2 to avoid the multiphoton absorption from diamonds. The $\Delta T/T_0$ signal of DAC with only the PTM under high pressure was also examined, and no signal was observed. To inspect the decompression effects for large-scale sample, a high-quality single-crystal GaAs wafer with ~1.5×2.5 mm size and ~0.5 mm thickness was compressed at 7 GPa at room temperature in a multi-anvil press (MAP) and then was unloaded from the MAP apparatus. The TRTS measurement for this pre-compressed sample was taken at ambient conditions. The experimental detail of the MAP was previously described [35].

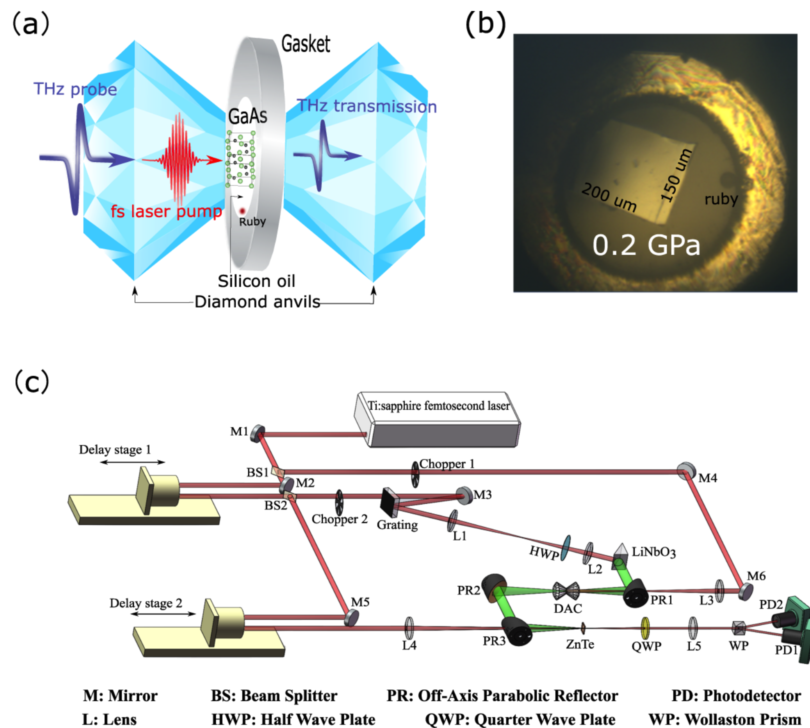

Fig. 1. (a) Schematic of the DAC for in-situ TRTS. (b) Morphology of the sample in the pressure chamber at 0.2 GPa. (c) Optical layout of the TRTS setup.

3. Results and discussion

3.1. Pressure tuning on interband photocarrier dynamics

The THz waveform passing through DAC without photoexcitation under an initial pressure of 0.2 GPa is shown in Fig. 2(a). The corresponding spectrum is plotted in the inset. It worth noting that the THz-electric-field induced nonlinear absorption in photoexcited GaAs should be negligible because about 90% of THz energies are blocked by the DAC apparatus. The normalized -$\Delta T/T_0$, proportional to the THz photoconductivity change, for GaAs at ambient

pressure is displayed in Fig. 2(b), in agreement with a single exponential function with a lifetime of approximately 4 ns. Figure 2(c) presents the transient -$\Delta T/T_0$ within a 22 ps time window under different pressures at an excitation fluence of 1.3 μJ/cm^2. The amplitude of -$\Delta T/T_0$ is significantly reduced with increasing pressure and approaches zero above 2 GPa. It is illustrated more clearly in Fig. 2(d), which plots the maximum amplitude of -$\Delta T/T_0$ as the function of pressure. One can see that the amplitude is attenuated by an order of magnitude as the pressure exceeds 2 GPa. The direct bandgap of GaAs is 1.65 eV at 2 GPa, beyond the 800 nm (1.55 eV) photon energy, as calculated by the empirical pressure coefficient of the bandgap of GaAs, i.e., $E(eV) = 1.4 \pm 0.01 + (0.125 \pm 0.005)P - (3.7 \pm 0.5)10^{-3}P^2$ [25]. Thus, under high pressure, the direct single-photon transition between the valence band and conduction band should be less efficient and can account for the significant pressure-induced decrease of -$\Delta T/T_0$.

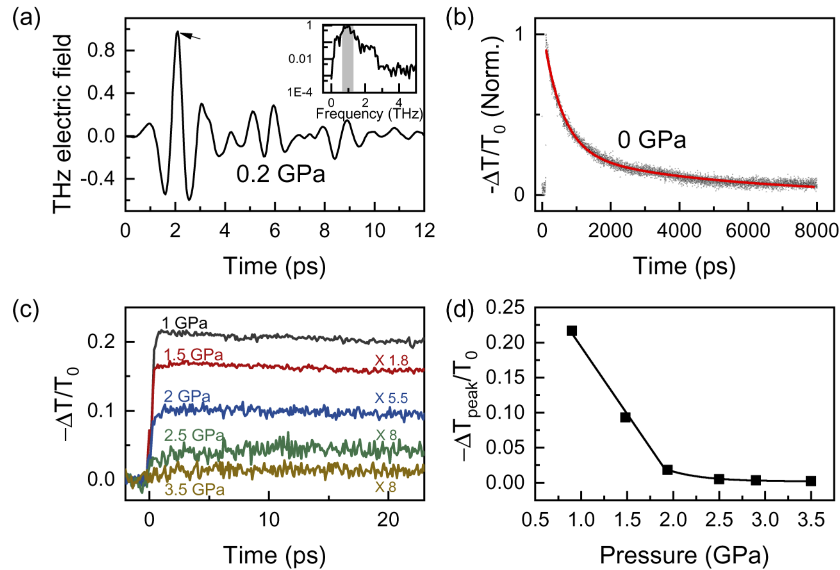

Fig. 2. (a) Transmitted THz waveform of the GaAs without optical photoexcitation at 0.2 GPa, where the THz main peak is denoted by the arrow. The corresponding frequency spectrum is plotted in the inset. (b) Normalized -$\Delta T/T_0$ as the function of pump-probe delay for GaAs at ambient pressure. The black circle and red line are the experimental data and the fitting curve using an exponential equation, respectively. (c) -$\Delta T/T_0$ transients at different pressures. For comparison, the curve at 1.5, 2, 2.5 and 3 GPa is scaled up by 1.8, 5.5, 8 and 8 times, respectively. (d) Peak value of -$\Delta T/T_0$ as the function of pressure.

The applied pump fluence is raised to 20 μJ/cm^2 to access the photocarrier dynamics under a higher pressure range, allowing for the interband excitation via two-photon absorption, as discussed later. The normalized -$\Delta T/T_0$ curves obtained between 2.5 GPa and 10 GPa are shown in Fig. 3(a). The decay, indicating the interband photocarrier relaxation, becomes faster under higher pressure. The relaxation dynamics can be well reproduced using single exponential functions with additional offsets below 4 GPa. However, double exponential functions are required to obtain a proper fit under higher pressure. The extracted average lifetime under different pressures is displayed in Fig. 3(b). It can be seen that the lifetime is significantly reduced from about 4 ns at ambient conditions to 65 ps under a pressure of 10 GPa, showing a decrease of nearly two orders of magnitude. Furthermore, we investigate the pump fluence dependence of photocarrier dynamics at 10 GPa by varying the pump level from 11 to 53 μJ/cm^2 as shown in Fig. 3(c). Correspondingly, the maximum amplitude of -$\Delta T/T_0$, as a function of the pump fluence, is consistent with a power function with a factor of 1.3, as displayed in the inset. This

nonlinear increasing trend with pump fluence can verify the existence of double photon transition [36] and explain the photoexcitation induced by pump photons with energy below the bandgap under high pressure. The pump-fluence-dependent time constants for the fast and slow decay components, τ_f and τ_s, are shown in Fig. 3(d). The τ_f is increased while the τ_s is decreased with elevating pump level. The reduction of τ_s may indicate that the Auger recombination process plays important role in the case of high photoexcitation level [37]. However, the pump-fluence dependence of τ_f implies that the fast decay stems from surface defect trapping [38]. The defect-related relaxation pathway normally gives rise to the augment of the photocarrier lifetime at a high photoexcitation level in view of the filling effects, that is, the available defect trapping channels should be decreased with the increasing number of photocarriers due to the constant density of defects [39]. It is known that the external pressure can facilitate the formation of surface defects in semiconductors [40,41], and therefore increase the density of nonradiative recombination centers, which leads to the fast trapping of photocarriers under high pressure. Therefore, this defect-assisted relaxation pathway should be responsible for the pressure-induced reduction of photocarrier lifetime. Other factors such as the variety of penetration depth of the pump beam and band bending may also affect the photocarrier relaxation under pressure due to the changes of band structure. Moreover, the photocarrier lifetime keeps as short as 57 picoseconds even the external pressure is totally released as shown in the inset of Fig. 3(b). This fact indicates that the pressure-induced defects in GaAs are irreversible. Furthermore, MAP is used to examine the decompression effect of photocarrier dynamics for mm-scale large-sized GaAs, by which the sample (~1.5×2.5 mm) is first compressed under 7 GPa before taking the TRTS measurement. One can see that the lifetime can be reduced to 5.5 ps, which is quite comparable with that in LT-GaAs [31]. It is worth noting that the GaAs compressed by MAP under 7 GPa has much shorter lifetime than by DAC under 10 Gpa. This anomaly should be ascribed to the non-hydrostatic pressure condition in MAP.

3.2. Pressure tuning on intraband photocarrier dynamics

Now we turn to the discussions on the rising processes of -$\Delta T/T_0$ under pressure, which contain intraband photocarrier dynamics such as intravalley cooling and intervalley scatterings [29]. Figure 4(a) focuses on the -$\Delta T/T_0$ transients within the time window of 20 ps. At ambient pressure, the -$\Delta T/T_0$ signal features an initial fast rising, and subsequently approaches maximum within the subpicosecond time scale, implying the completion of intraband photocarrier cooling and temporal peaking of THz photoconductivity. As increasing pressure, the initial growing process slows down, which is prolonged to almost 10 ps under 2.5 GPa. Then, it becomes relatively shortened when the pressure is increased above 3.5 GPa. We propose that the pressure behaviors of rising processes of -$\Delta T/T_0$ have close correspondences with the intervalley scatterings in GaAs. If the photo-injected electrons have excess kinetic energies larger than the threshold between energy valleys, e.g., the extreme points of the Γ and L valleys, a fraction of the electrons in the Γ valley can transfer into the neighboring (N) valley within tens of femtoseconds via LO phonon scattering followed by a slower returning process of several picoseconds. Such intervalley scattering tends to decrease the carrier mobility and relax the initial rising process of THz photoconductivity due to the larger effective mass in the N valley [42]. At ambient pressure, the fast rising dynamics is dominated by the intravalley cooling because the direct photoexcitation with 800 nm cannot provide excess energy above the intervalley threshold. However, under high pressure, the electrons scattering between the Γ and N valleys (including the L and X valleys) in GaAs should take place due to two-photon absorption (~ 3.1 eV photon energy), as mentioned above, and therefore contribute to the intraband carrier cooling. For example, from the estimations of electronic structures under pressure [25,43], the direct bandgap of GaAs is about 1.67 eV under 2.5 GPa, so the conduction band electrons injected with two phonon excitations can gain excess energy of more than 0.72 eV, far above the Γ-L energy difference of 0.17 eV, as

Optics EXPRESS

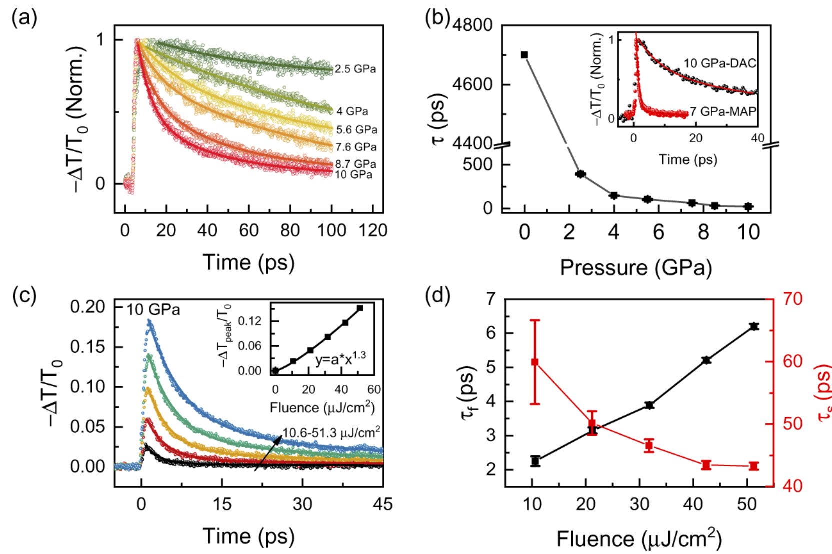

Fig. 3. (a) Normalized -$\Delta T/T_0$ of GaAs with 800 nm photoexcitation under different pressures. Solid lines are the fitting curves using exponential functions. (b) Average lifetime constant corresponding to interband relaxations as the function of pressure. The inset plot the -$\Delta T/T_0$ signal of unloaded GaAs sample from DAC (10 GPa) and Multi-anvil press (7 GPa), respectively. The applied pump fluence is about 2.0 μJ/cm^2. (c) -$\Delta T/T_0$ at different pump fluences. The solid lines are the fitting results using the exponential functions. Inset is the peak value of -$\Delta T/T_0$ at different fluences. (d) Pump fluence dependences of fast (black line), τ_f, and slow decay time (red line), τ_s, fitted by the exponential equations.

illustrated by Fig. 4(b). Since both the Γ and L valleys move upward with increasing external pressure, while the X valley behaves oppositely, e.g., as P= 3.5 GPa, Γ=1.86 eV, and X=1.851 eV, the Γ-X valley scattering should play a nontrivial role with further increasing pressure. However, the extreme point of the X valley is lower than that of the Γ valley, and an indirect band structure forms when the pressure exceeds 4 GPa. As a result, the electrons scattering to the X valley cannot go back to the Γ valley. Instead, they recombine with defects or holes directly, as shown in Fig. 4(c). Consequently, the rising processes of -$\Delta T/T_0$ essentially remain constant and are less sensitive to the external pressure above 5 GPa.

We also measured the -$\Delta T/T_0$ signal using a photoexcitation with a 600 nm wavelength, ensuring that the photocarrier has excess energy larger than the Γ-L threshold (see Fig. 4(d)). The initial rising time is pronouncedly delayed compared with that photoexcited by 800 nm under ambient pressure, emphasizing the occurrence of intervalley scattering. As illustrated in Fig. 4(e) and (f), the band gap further opens, and the excess energy of photocarrier is expected to reduce with increasing pressure. Consequently, the intervalley scattering effect begins to fade, and the rising process of -$\Delta T/T_0$ signal speeds up under higher pressure.

Furthermore, the intraband photocarrier dynamics under pressure are quantitatively investigated using the well-established three-state model [31,44,45]. In this model, electronic states in the Γ valley are separated into Γ+ and Γ− energy levels as shown in Fig. 4(b), only the electrons in Γ+ state can energetically transfer into N valleys. The electronic states in the N valley are set as the third state, in which the electrons can only scatter into the Γ+ state. Meanwhile, the Γ− electrons are relaxed to the bottom of CB through intravalley inelastic phonon scattering. The populations

Optics EXPRESS

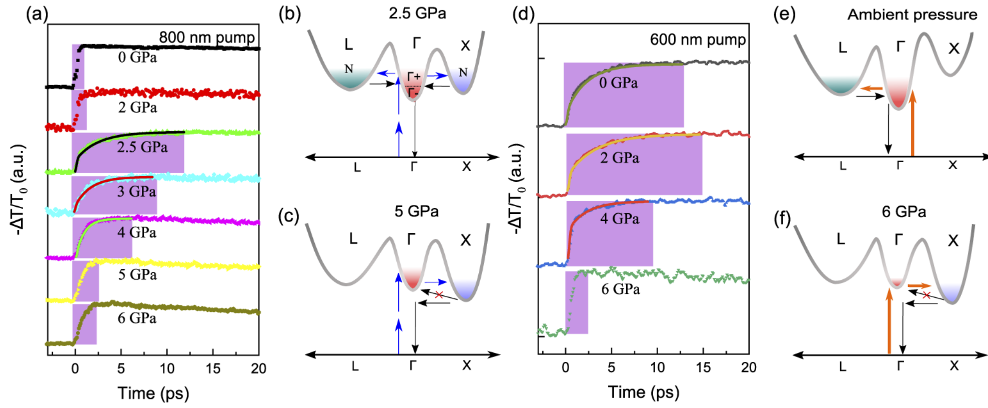

Fig. 4. (a) and (d) Normalized -$\Delta T/T_0$ in the short time range of 20 ps for photoexcitation at 800 nm and 600 nm respectively. The curves are shifted vertically for comparison. The solid circles and solid lines represent the experimental data and fitting results using the three state model, respectively. The shaded area indicates the rising process of the signal. (b), (c), (e) and (f) Schematic of the electronic band structure of GaAs and related intervalley scattering mechanism. (b) and (c) represent the photoexcitation condition with 800 nm at 2.5 and 5 GPa, respectively. (e) and (f) correspond to the photoexcitation using 600 nm at ambient pressure and 6 GPa, respectively.

of electrons in Γ+, Γ− and N state are determined by the three-state rate equations

$$\frac{dN_{\Gamma+}(t)}{dt} = \frac{I_0\alpha}{hv}I(t) - (\frac{1}{\tau_{\Gamma N}} + \frac{1}{\tau_\Delta})N_{\Gamma+}(t) + \frac{1}{\tau_{N\Gamma}}N_N(t), \tag{1}$$

$$\frac{dN_N(t)}{dt} = \frac{1}{\tau_{\Gamma N}}N_{\Gamma+}(t) - \frac{1}{\tau_{N\Gamma}}N_N(t), \tag{2}$$

$$\frac{dN_{\Gamma-}(t)}{dt} = \frac{1}{\tau_\Delta}N_{\Gamma+}(t). \tag{3}$$

Here, $N_{\Gamma+}(t), N_N(t)$ and $N_{\Gamma-}(t)$ represent the number of electrons in the Γ+, N and Γ− state, respectively. An excitation term corresponding to the pump pulse with temporal Gaussian shape, $I(t) = I_0exp(-\frac{t^2}{\tau_d^2})$, is introduced. $\tau_d = 45fs$ is the pump pulse duration. α is the interband absorption coefficient, and hv is photon energy. $\tau_{\Gamma N}$, τ_Δ and $\tau_{N\Gamma}$ denote the average scattering time of Γ+ ⟶ N (L or X), Γ+ ⟶ Γ−, and N ⟶ Γ processes, respectively. It is known that -$\Delta T/T_0$ is proportional to the photoinduced change in the real part of THz conductivity [46]. Because the Γ-valley electron has a far smaller effective mass than that in the L- (or X-) valley, we only take into account the Γ-valley contribution to the carrier mobility. Thereby, the normalized -$\Delta T/T_0$ with respect to its maximum can be simplified as

$$-\frac{\Delta T}{T_0}(Norm.) = \frac{N_{\Gamma+}(t) + N_{\Gamma-}(t)}{N_0}. \tag{4}$$

Here, N_0 denotes the maximum photoexcited carrier density. It should be mentioned that the nonparabolic effect of the Γ valley is neglected in the calculations. As shown in Fig. 4(a) and (d), the good agreement between calculated and experimental $-\Delta T/T_0(Norm.)$ curves can be seen, whereby the dynamic parameters are extracted and summarized in Table 1. One can see that the intravalley cooling time of the Γ valley characterized with τ_Δ changes slightly (110-140 fs) for different pressures. The obtained Γ ⟶ N valley (Γ ⟶ N) scattering time, $\tau_{\Gamma N}$, falls in the 30-60

Optics EXPRESS

fs time scale under high pressure, consistent with the earlier reported result (50 fs) based on the three-state model in GaAs at ambient condition [44]. The scattering process from the N valleys to Γ (N → Γ) is highly pressure-dependent, e.g., the $\tau_{N\Gamma}$ decreases from 0.81 ps to 0.2 ps in the range of 2.5-4 GPa, which is related to both the L and X valley intervalley scatterings. Such pressure behavior could be attributed to the varieties of energy band structures.

Table 1. Fitting parameters of $\tau_{N\Gamma}$, τ_{Δ}, $\tau_{\Gamma N}$ fitted by the three-state model at photoexcitation at 800 nm and 600 nm at different pressures.

Wavelength	P (GPa)	$\tau_{N\Gamma}$ (ps)	τ_{Δ} (ps)	$\tau_{\Gamma N}$ (ps)
800 nm	2.5	0.81±0.1	0.11±0.05	0.06±0.05
	3.5	0.34±0.08	0.14±0.05	0.04±0.05
	4	0.2±0.06	0.1±0.05	0.03±0.05
600 nm	0	0.8±0.12	0.12±0.05	0.06±0.05
	2	0.85±0.1	0.14±0.05	0.06±0.05
	4	0.57±0.08	0.13±0.05	0.11±0.05

Firstly, the effective mass of the Γ valley in GaAs increases with pressure [47], indicating a large density of states under high pressure. It means that the available phase space for the N → Γ scattering increases with pressure and accelerates the return scattering processes. Secondly, more phonon modes with large q would be enabled to participate in the intervalley scattering as the minima energy of band valleys changes with pressure [48], which will decrease the N → Γ scattering time as well. For photoexcitation at 600 nm, only the Γ- L valley scattering participates at ambient pressure. The N → Γ time constant increases marginally around 2 GPa, while decreasing to 0.57 ps under 4 GPa. Compared with photoexcitation at 800 nm through

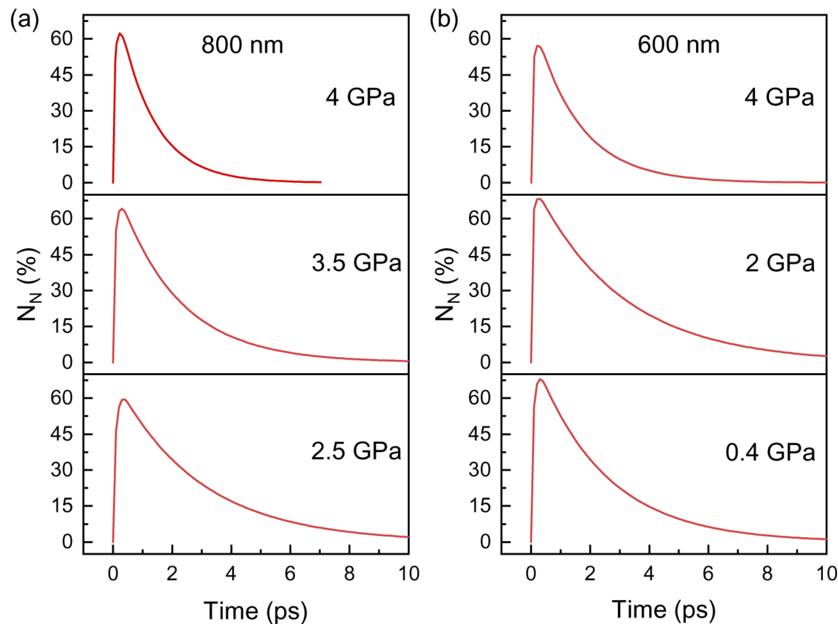

Fig. 5. Fraction of photoexcited electrons transferred to neighboring valleys (N_N) as a function of time according to the three-state model calculations under different pressures with (a) 800 nm and (b) 600 nm photoexcitation, respectively.

two-photon transition, the 600 nm single-photon excitations provide relatively small excess energies above the conduction band minima for electrons, and therefore less optical phonon modes assisting the N → Γ scattering can be activated. As a result, the N → Γ scattering time constant is larger than that under photoexcitation at 800 nm and 4 GPa. In addition, the population ratio (N_N) of hot carriers transferred to N valleys at different pressures is extracted using the fitting parameters, which is shown in Fig. 5. The N_N curve can be described by a fast-rising process followed by a slow decay in a few ps time scale, which agrees with the pressure effects, as shown in Fig. 4. Notably, the depopulation time of the N-valley electrons originated from the competing transfer processes between the Γ + → Γ− and N → Γ, is far longer than the intervalley scattering time constant, $\tau_{N\Gamma}$ [45]. On the other hand, the N-valley electron fraction is larger than 60%, emphasizing more electrons take part in intervalley scattering than that in intravalley cooling. It is reasonable since the obtained time constants of Γ → N scattering are shorter than that of intravalley scattering under high pressure, i.e., the Γ → N scattering rate is faster than the intravalley relaxation rate of the Γ valley electrons.

4. Conclusions

In summary, photocarrier dynamics in GaAs under hydrostatic pressure up to 10 GPa using TRTS with a DAC are studied. The intense THz source from an $LiNbO_3$ crystal overcomes the drastic attenuations from the DAC and gives access to the nonequilibrium carrier dynamics such as interband relaxation and intervalley scattering. The THz photoconductivity lifetime associated with interband relaxation is found to drop to a few picoseconds at high pressures compared with the nanosecond time scale under ambient pressure. Such significant decrease of two orders of magnitude in the photocarrier lifetime can be understood in terms of the pressure-induced augmentation in the density of surface defect states. Meanwhile, the pressure effects on the intraband carrier cooling are observed. Based on the three state equations, the intervalley scattering time constants are obtained from the transient THz transmission under different pressure. The scattering time from neighboring valleys to the Γ valley is reduced nearly four-fold as the pressure increases from 2 GPa to 4 GPa, in agreement with the change of conduction band structure with pressure. This research provides a new perspective to examine the photocarrier dynamics in semiconductors using high-pressure THz spectroscopy. It is valuable for tailoring the photocarrier lifetime of GaAs under high pressure, which is essential for developing GaAs-based high-speed photoelectric devices.

Funding. National Natural Science Foundation of China (11774354, 11874361, 12004387, 51672279, 51727806, 61988102); Science Challenge Project (TZ2016001); Chinese Academy of Sciences Innovation Grant (CXJJ-19-B08); Hefei Institutes of Physical Science, Chinese Academy of Sciences (CASHIPS) Director Fund (YZJJ201705).

Disclosures. The authors declare no conflicts of interest.

References

1. H.-H. Fang, S. Adjokatse, S. Shao, J. Even, and M. A. Loi, "Long-lived hot-carrier light emission and large blue shift in formamidinium tin triiodide perovskites," Nat. Commun. **9**(1), 243 (2018).
2. Y. Zhang, H. Li, L. Wang, H. Wang, X. Xie, S.-L. Zhang, R. Liu, and Z.-J. Qiu, "Photothermoelectric and photovoltaic effects both present in MoS_2," Sci. Rep. **5**(1), 7938 (2015).
3. M. V. Fischetti, D. J. DiMaria, S. D. Brorson, T. N. Theis, and J. R. Kirtley, "Theory of high-field electron transport in silicon dioxide," Phys. Rev. B **31**(12), 8124–8142 (1985).
4. Y. C. Shen, P. C. Upadhya, E. H. Linfield, H. E. Beere, and A. G. Davies, "Ultrabroadband terahertz radiation from low-temperature-grown GaAs photoconductive emitters," Appl. Phys. Lett. **83**(15), 3117–3119 (2003).
5. S. Gupta, J. F. Whitaker, and G. A. Mourou, "Ultrafast carrier dynamics in III-V semiconductors grown by molecular-beam epitaxy at very low substrate temperatures," IEEE J. Quantum Electron. **28**(10), 2464–2472 (1992).
6. F. E. Doany, D. Grischkowsky, and C. C. Chi, "Carrier lifetime versus ion-implantation dose in silicon on sapphire," Appl. Phys. Lett. **50**(8), 460–462 (1987).
7. H. Esmaielpour, K. R. Dorman, D. K. Ferry, T. D. Mishima, M. B. Santos, V. R. Whiteside, and I. R. Sellers, "Exploiting intervalley scattering to harness hot carriers in III-V solar cells," Nat. Energy **5**(4), 336–343 (2020).
8. Y. Yang, D. P. Ostrowski, R. M. France, K. Zhu, J. van de Lagemaat, J. M. Luther, and M. C. Beard, "Observation of a hot-phonon bottleneck in lead-iodide perovskites," Nat. Photonics **10**(1), 53–59 (2016).

9. J. Yang, X. Wen, H. Xia, R. Sheng, Q. Ma, J. Kim, P. Tapping, T. Harada, T. W. Kee, F. Huang, Y.-B. Cheng, M. Green, A. Ho-Baillie, S. Huang, S. Shrestha, R. Patterson, and G. Conibeer, "Acoustic-optical phonon up-conversion and hot-phonon bottleneck in lead-halide perovskites," Nat. Commun. **8**(1), 14120 (2017).
10. J. Fu, Q. Xu, G. Han, B. Wu, C. H. A. Huan, M. L. Leek, and T. C. Sum, "Hot carrier cooling mechanisms in halide perovskites," Nat. Commun. **8**(1), 1300 (2017).
11. M. Li, S. Bhaumik, T. W. Goh, M. S. Kumar, N. Yantara, M. Grätzel, S. Mhaisalkar, N. Mathews, and T. C. Sum, "Slow cooling and highly efficient extraction of hot carriers in colloidal perovskite nanocrystals," Nat. Commun. **8**(1), 14350 (2017).
12. H.-K. Mao, X.-J. Chen, Y. Ding, B. Li, and L. Wang, "Solids, liquids, and gases under high pressure," Rev. Mod. Phys. **90**(1), 015007 (2018).
13. J. M. Pietryga, K. K. Zhuravlev, M. Whitehead, V. I. Klimov, and R. D. Schaller, "Evidence for Barrierless Auger Recombination in PbSe Nanocrystals: A Pressure-Dependent Study of Transient Optical Absorption," Phys. Rev. Lett. **101**(21), 217401 (2008).
14. X. Meng, T. Pandey, J. Jeong, S. Fu, J. Yang, K. Chen, A. Singh, F. He, X. Xu, J. Zhou, W.-P. Hsieh, A. K. Singh, J.-F. Lin, and Y. Wang, "Thermal Conductivity Enhancement in MoS_2 under Extreme Strain," Phys. Rev. Lett. **122**(15), 155901 (2019).
15. K. Ni, J. Du, J. Yang, S. Xu, X. Cong, N. Shu, K. Zhang, A. Wang, F. Wang, L. Ge, J. Zhao, Y. Qu, K. S. Novoselov, P. Tan, F. Su, and Y. Zhu, "Stronger Interlayer Interactions Contribute to Faster Hot Carrier Cooling of Bilayer Graphene under Pressure," Phys. Rev. Lett. **126**(2), 027402 (2021).
16. F. H. Su, F. Blanchard, G. Sharma, L. Razzari, A. Ayesheshim, T. L. Cocker, L. V. Titova, T. Ozaki, J. C. Kieffer, R. Morandotti, M. Reid, and F. A. Hegmann, "Terahertz pulse induced intervalley scattering in photoexcited GaAs," Opt. Express **17**(12), 9620–9629 (2009).
17. G. Sharma, I. Al-Naib, H. Hafez, R. Morandotti, D. G. Cooke, and T. Ozaki, "Carrier density dependence of the nonlinear absorption of intense THz radiation in GaAs," Opt. Express **20**(16), 18016–18024 (2012).
18. H. J. Shin, V. L. Nguyen, S. C. Lim, and J.-H. Son, "Ultrafast nonlinear travel of hot carriers driven by high-field terahertz pulse," J. Phys. B: At., Mol. Opt. Phys. **51**(14), 144003 (2018).
19. P. Bowlan, W. Kuehn, K. Reimann, M. Woerner, T. Elsaesser, R. Hey, and C. Flytzanis, "High-Field Transport in an Electron-Hole Plasma: Transition from Ballistic to Drift Motion," Phys. Rev. Lett. **107**(25), 256602 (2011).
20. R. Ulbrich, "Energy Relaxation of Photoexcited Hot Electrons in GaAs," Phys. Rev. B **8**(12), 5719–5727 (1973).
21. M. Heiblum, M. I. Nathan, D. C. Thomas, and C. M. Knoedler, "Direct Observation of Ballistic Transport in GaAs," Phys. Rev. Lett. **55**(20), 2200–2203 (1985).
22. P. Y. Yu and B. Welber, "High pressure photoluminescence and resonant Raman study of GaAs," Solid State Commun. **25**(4), 209–211 (1978).
23. M. Boucenna and N. Bouarissa, "Predicted electronic properties of GaAs under hydrostatic pressure," Mater. Chem. Phys. **84**(2-3), 375–379 (2004).
24. R. J. Almassy, D. C. Reynolds, C. W. Litton, K. K. Bajaj, and G. L. McCoy, "Observation of shallow residual donors in high purity epitaxial GaAs by means of photoluminescence spectroscopy," Solid State Commun. **38**(11), 1053–1056 (1981).
25. M. Leroux, G. Pelous, F. Raymond, and C. Verie, "Minority-carrier lifetime study of the pressure induced Γ-X crossover in GaAs," Appl. Phys. Lett. **46**(3), 288–290 (1985).
26. M. Leroux, P. Gibart, J. M. Sallese, and C. Verie, "High-pressure dependence of the room-temperature minority carrier lifetimes in GaAs," Semicond. Sci. Technol. **4**(4), 233–234 (1989).
27. M. Leroux, J. M. Sallese, J. Leymarie, G. Neu, and P. Gibart, "High-pressure photoluminescence study of GaAs doped with various donor species," Semicond. Sci. Technol. **6**(6), 514–517 (1991).
28. P. Grivickas, M. D. McCluskey, and Y. M. Gupta, "Order-of-magnitude reduction of carrier lifetimes in [100] n-type GaAs shock-compressed to 4 GPa," Appl. Phys. Lett. **98**(9), 092107 (2011).
29. M. C. Nuss, D. H. Auston, and F. Capasso, "Direct Subpicosecond Measurement of Carrier Mobility of Photoexcited Electrons in Gallium Arsenide," Phys. Rev. Lett. **58**(22), 2355–2358 (1987).
30. M. C. Beard, G. M. Turner, and C. A. Schmuttenmaer, "Transient photoconductivity in GaAs as measured by time-resolved terahertz spectroscopy," Phys. Rev. B **62**(23), 15764–15777 (2000).
31. M. C. Beard, G. M. Turner, and C. A. Schmuttenmaer, "Subpicosecond carrier dynamics in low-temperature grown GaAs as measured by time-resolved terahertz spectroscopy," J. Appl. Phys. **90**(12), 5915–5923 (2001).
32. M. Nagai and M. Kuwata-Gonokami, "Time-resolved reflection spectroscopy of the spatiotemporal dynamics of photo-excited carriers in Si and GaAs," J. Phys. Soc. Jpn. **71**(9), 2276–2279 (2002).
33. J. A. Fülöp, L. Pálfalvi, G. Almási, and J. Hebling, "Design of high-energy terahertz sources based on optical rectification," Opt. Express **18**(12), 12311–12327 (2010).
34. H. Hirori, A. Doi, F. Blanchard, and K. Tanaka, "Single-cycle terahertz pulses with amplitudes exceeding 1 MV/cm generated by optical rectification in $LiNbO_3$," Appl. Phys. Lett. **98**(9), 091106 (2011).
35. H. Tang, X. Gao, J. Zhang, B. Gao, W. Zhou, B. Yan, X. Li, Q. Zhang, S. Peng, D. Huang, L. Zhang, X. Yuan, B. Wan, C. Peng, L. Wu, D. Zhang, H. Liu, L. Gu, F. Gao, T. Irifune, R. Ahuja, H.-K. Mao, and H. Gou, "Boron-Rich Molybdenum Boride with Unusual Short-Range Vacancy Ordering, Anisotropic Hardness, and Superconductivity," Chem. Mater. **32**(1), 459–467 (2020).

Optics EXPRESS

36. J. K. Wahlstrand and E. J. Heilweil, "Contactless THz-based bulk semiconductor mobility measurements using two-photon excitation," Opt. Express **26**(23), 29848–29853 (2018).
37. H. Mariette, D. J. Wolford, and J. A. Bradley, "Time decays of donor-bound excitons in GaAs under pressure-induced Γ-X crossover," Phys. Rev. B **33**(12), 8373–8378 (1986).
38. P. Uhd Jepsen, W. Schairer, I. H. Libon, U. Lemmer, N. E. Hecker, M. Birkholz, K. Lips, and M. Schall, "Ultrafast carrier trapping in microcrystalline silicon observed in optical pump-terahertz probe measurements," Appl. Phys. Lett. **79**(9), 1291–1293 (2001).
39. F. Ceballos, Q. Cui, M. Z. Bellus, and H. Zhao, "Exciton formation in monolayer transition metal dichalcogenides," Nanoscale **8**(22), 11681–11688 (2016).
40. A. Misiuk, "Evolution of Process - Induced Defects in Silicon under Hydrostatic Pressure," in *Gettering and Defect Engineering in Semiconductor Technology IV*, vol. 19 of *Solid State Phenomena* (Trans Tech Publications Ltd, 1991), pp. 387–392.
41. G. T. Gray, "Shock-Induced Defects in Bulk Materials," MRS Proc. **499**, 87–98 (1997).
42. S. E. Ralph, Y. Chen, J. Woodall, and D. McInturff, "Subpicosecond photoconductivity of $Ga_0.53As_0.47$: Intervalley scattering rates observed via THz spectroscopy," Phys. Rev. B **54**(8), 5568–5573 (1996).
43. M. Leroux, G. Neu, and C. Vèrié, "High pressure dependence of the electronic properties of bound states in n-type GaAs," Solid State Commun. **58**(5), 289–293 (1986).
44. C. J. Stanton and D. W. Bailey, "Rate equations for the study of femtosecond intervalley scattering in compound semiconductors," Phys. Rev. B **45**(15), 8369–8377 (1992).
45. S. Wu, P. Geiser, J. Jun, J. Karpinski, D. Wang, and R. Sobolewski, "Time-resolved intervalley transitions in GaN single crystals," J. Appl. Phys. **101**(4), 043701 (2007).
46. M. R. Bergren, B. J. Simonds, B. Yan, G. Yue, R. Ahrenkiel, T. E. Furtak, R. T. Collins, P. C. Taylor, and M. C. Beard, "Electron transfer in hydrogenated nanocrystalline silicon observed by time-resolved terahertz spectroscopy," Phys. Rev. B **87**(8), 081301 (2013).
47. Z. X. Jiang, R. J. Chen, J. G. Tischler, B. A. Weinstein, and B. D. McCombe, "Pressure Dependence of the Electron Effective Mass in GaAs up to the 1s(Γ)-1s(X) Crossover," phys. stat. sol. (b) **198**(1), 41–47 (1996).
48. N. Tandon, L. R. Ram-Mohan, and J. D. Albrecht, "Effect of hydrostatic pressure on the electron-phonon scattering in GaAs," J. Appl. Phys. **126**(1), 015701 (2019).